FRACTURE RELATED CROSS-OVER FREQUENCIES OF SEISMIC ATTENUATION IN POROUS ROCKS

M. Brajanovski, T.M. Müller, and B. Gurevich

email: *tobias.mueller@gpi.uni-karlsruhe.de*

keywords: *Wave-induced flow, seismic attenuation, fractured rocks, diffusion*

ABSTRACT

We analyze compressional wave attenuation in fluid-saturated porous material with porous inclusions having different compressibility and very different spatial scale in comparison with the background. Such a medium exhibits attenuation due to wave-induced fluid flow across the interface between inclusion and background. We show that overall wave attenuation is governed by the superposition of two coupled fluid-diffusion processes. Associated with two characteristic spatial scales, we compute two cross-over frequencies that separate three different frequency regimes. We give a physical explanation for an intermediate range of frequencies, where attenuation scales with $\omega^{1/2}$. The potential application of this model is in estimation of the background permeability as well as inclusion scale (thickness) by identifying these frequencies from the attenuation measurement.

INTRODUCTION

One of the main intrinsic seismic wave dissipation mechanisms is associated with the wave-induced flow of the pore fluid. This effect occurs in a heterogeneous porous medium when a passing wave induces a local pressure gradient on the interface between inclusion and the background. In order to equilibrate pressure, viscous fluid moves across the interface (Pride and Berryman, 2003; Pride et al., 2004; Brajanovski et al., 2005).

In all these studies similar general behavior of attenuation versus frequency is observed. In particular, for high contrast in permeabilities, compressibilities and spatial scales between inclusion and background, three different frequency regimes can be identified. Dimensionless attenuation (inverse quality factor) is proportional to the first power of frequency ω at low frequencies, to $\omega^{-1/2}$ at high frequencies, and to $\omega^{1/2}$ in the intermediate frequency range, see Figure 1. However, the physical description how induced diffusion fluid motion produces intermediate frequency range, remains unclear.

In this paper we show that the intermediate frequency regime is a general feature of saturated porous media with two very distinct elastic properties of the inclusion and the background and two very different characteristic length scales that are 1) scale of the inclusions and 2) distance between them. Based on the dispersion equation for the effective P-wave modulus for porous fractured rocks (Brajanovski et al., 2005), we compute two cross-over frequencies that separate three different frequency regimes of attenuation. In order to give physical explanation for the intermediate $\omega^{1/2}$ frequency dependency, we show that overall wave attenuation is governed by two coupled fluid diffusion processes.

ATTENUATION OF P-WAVE IN FRACTURED ROCK

Brajanovski et al (Brajanovski et al., 2005) showed that effective frequency-dependent, fluid-saturated P-wave modulus $c_{33}^{sat}(\omega)$ of porous rock with periodic system of fractures parallel to x_1x_2 plane with spatial

period H is given by

$$\frac{1}{c_{33}^{sat}} = \frac{1}{C_b} + \frac{\Delta_N \left(R_b - 1\right)^2}{L_b \left[1 - \Delta_N + \Delta_N \sqrt{i\Omega} \cot\left(\frac{C_b}{M_b}\sqrt{i\Omega}\right)\right]} , \tag{1}$$

where Δ_N is the fracture weakness (Hsu and Schoenberg, 1993; Bakulin et al., 2000) of value between 0 and 1, defined by $\Delta_N = Z_N L_b/(1 + Z_N L_b)$. $Z_N = \lim_{h_c \to 0}(h_c/L_c)$ is the normal excess compliance describing fracture contribution in compliance matrix in the linear-slip deformation theory (Schoenberg and Douma, 1988). Index c denotes fracture parameters while index b denotes parameters of the porous background. In equation (1) Ω is the normalized frequency given by

$$\Omega = \omega \frac{H^2 M_b^2}{4 C_b^2 D_b^2} . \tag{2}$$

The background material is specified by fluid-saturated P-wave velocity modulus C_b, diffusivity $D_b = \kappa_b M_b L_b/\eta C_b$, permeability κ_b, pore space modulus M_b, dry (drained) P-wave modulus L_b, material parameter $R_b = \alpha_b M_b/C_b$ and Biot-Willis coefficient α_b. Viscosity of the fluid is η. The complex P-wave velocity is $V_{p3} = \sqrt{c_{33}^{sat}/\rho_b}$, where $\rho_b = \rho_g(1 - \phi_b) + \rho_f \phi_b$ is mass density of the fluid-saturated background material. The P-wave phase velocity is $V_p = \left[\mathrm{Re}\left(\mathrm{V}_{\mathrm{p3}}^{-1}\right)\right]^{-1}$and the attenuation Q^{-1} is given by $Q^{-1} = 2V_p \mathrm{Im}\left(\mathrm{V}_{\mathrm{p3}}^{-1}\right)$.

Expression (1) is valid for frequencies much smaller than Biot's characteristic frequency (fluid flow in the pore channels is Poiseuille flow), and also much smaller than the resonant frequency of the layering (effective medium approximation is valid). Within these conditions, we can still define low and high frequencies with respect to fluid flow. Low frequencies are those when pressure has enough time to equilibrate between layers within the wave cycle, while for high frequencies this is not possible.

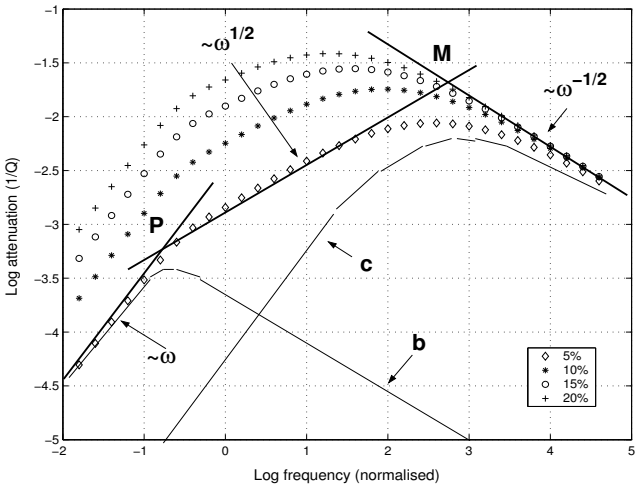

Figure 1: *Log-log plot of attenuation versus circular frequency for water saturated quartz grained sandstone ($K_g = 37$ GPa, $\mu_g = 44$ GPa, $\rho_g = 2.65$ g·cm^{-1}) of porosity $\phi = 0.2$ and fracture weakness Δ_N in range from 0.05 up to 0.2. Three different asymptotic parts of the attenuation curves are observed.*

ASYMPTOTIC ANALYSIS

In Figure 1, where $\log(Q^{-1})$ is plotted versus $\log\omega$, we observe that the normalized frequency for peak attenuation decreases with increasing fracture weakness Δ_N. In the high-frequency limit the attenuation is proportional to $\omega^{-1/2}$. In the low-frequency limit attenuation is proportional to ω. From the curve marked with diamonds, for the case of lower fracture weakness (which intuitively corresponds to "thinner" fractures), we clearly observe a transitional part proportional to $\omega^{1/2}$. Points P and M define cross-over frequencies separating attenuation behavior. We derive analytical expressions for the cross-over frequencies and investigate their dependence on fracture parameters.

From the definition of Q^{-1} and dispersion relation (1) we find asymptotic solution for imaginary parts of the complex velocity V_{p3} normalized by the constant real velocity $\sqrt{C_b/\rho_b}$. By using the expansion of $\cot z$ for small argument z low-frequency asymptote is

$$\mathrm{Im}\frac{1}{\mathrm{c}_{33}^{\mathrm{sat}}} = \mathrm{Im}\left\{\mathrm{T}\left[\frac{1}{\Delta_{\mathrm{N}}} - 1 + \sqrt{\mathrm{i}\Omega}\cot\left(\frac{\mathrm{C_b}}{\mathrm{M_b}}\sqrt{\mathrm{i}\Omega}\right)\right]^{-1}\right\} \approx \frac{\mathrm{T}\Omega\mathrm{C_b}}{3\mathrm{M_b}\mathrm{B}^2}\ , \tag{3}$$

where $T = L_b^{-1}\left(R_b - 1\right)^2$and $B = (1/\Delta_N + M_b/C_b - 1)$. Hence, Q^{-1} is proportional to ω.

To find the intermediate asymptote we have to analyze the double limit, first take the approximation for small fracture weakness and then take the limit as frequency goes to zero. Small Δ_N limit is obtained from equation (1) using

$$\mathrm{Im}\frac{1}{\mathrm{c}_{33}^{\mathrm{sat}}} = \mathrm{Im}\frac{\mathrm{T}\Delta_{\mathrm{N}}}{1 - \Delta_{\mathrm{N}} + \Delta_{\mathrm{N}}\mathrm{F}} \approx \mathrm{Im}\Delta_{\mathrm{N}}\mathrm{T}\left(1 + \Delta_{\mathrm{N}} - \Delta_{\mathrm{N}}\mathrm{F}\right) = \mathrm{T}\Delta_{\mathrm{N}}^2\mathrm{ImF}\ , \tag{4}$$

where $F = \sqrt{i\Omega}\cot(C_b\sqrt{i\Omega}/M_b)$. We calculate ImF by representing cotangent function of complex argument in exponential form and then expressing the result in terms of trigonometric and hyperbolic functions. As $\Omega \to 0$, taking only first term in expansion of ImF and then substituting ImF into equation (4) yields

$$\mathrm{Im}\frac{1}{\mathrm{c}_{33}^{\mathrm{sat}}} = \frac{\mathrm{T}\sqrt{\Omega}\Delta_{\mathrm{N}}^2}{2}\ . \tag{5}$$

The latter equation shows that in the double limit of small fracture weakness and low frequency Q^{-1} is proportional to $\omega^{1/2}$.

The lower cross-over frequency can be computed by looking at intersection of these two asymptotes. Equating right-hand sides of equations (3) and (5), and substituting $B^2 \approx 1/\Delta_N$ gives normalized crossover frequency $\Omega_P = \left(3M_b/2C_b\right)^2$ for point P. From equation (2) we calculate the corresponding real angular frequency ω_P

$$\omega_P = \frac{9D_b}{H^2}\ . \tag{6}$$

The high-frequency asymptote can be obtained in a similar way. Writing the cotangent function in exponential form and taking limit $\Omega \to \infty$ and $P \to \infty$, we get imaginary part of the modulus

$$\mathrm{Im}\frac{1}{\mathrm{c}_{33}^{\mathrm{sat}}} = \mathrm{Im}\frac{\mathrm{T}}{\frac{1}{\Delta_{\mathrm{N}}} - 1 - \frac{\mathrm{i}-1}{\sqrt{2}}\sqrt{\Omega}} \approx \frac{\mathrm{T}}{\sqrt{2\Omega}}\ , \tag{7}$$

thus, for high frequencies Q^{-1} is proportional to $\omega^{-1/2}$.

Equating right-hand sides of equations (7) and (5) gives the upper normalized cross-over frequency $\Omega_M = \sqrt{2}/\Delta_N^2$ (point M), which is an approximation for the maximum of attenuation. From equation (2), the corresponding real angular frequency ω_M is

$$\omega_M = 4\sqrt{2}D_b\left(\frac{C_b}{M_bH}\right)^2\Delta_N^{-2}\ . \tag{8}$$

COUPLED DIFFUSION

The attenuation behavior described in previous section can be interpreted as a superposition of two hypothetical diffusion processes (represented by curves b and c in Figure 1). Although, each layer alone does not produce any attenuation (because the layer is homogeneous), when connected together, attenuation takes place because the pore pressure gradient across the interface is induced. In order to equilibrate pressure, fluid flow occurs between layers (background and fracture). This process is described by the diffusion equation. Symmetry of the system causes no-flow condition in the middle of each layer. Intuitively, we can say that condition for maximal attenuation is when fluid penetrates layers to the maximal possible depth.

Let us analyze the process in the background. Cross-over frequency ω_P, given by equation (6) is independent of fracture weakness Δ_N but depends on the ratio between diffusivity and thickness of the

background. This is logical because diffusion length δ_c in fracture at this frequency is several orders of magnitude bigger than the thickness of fracture, such that it cannot control the frequency dependency of the relaxation process in the background. In other words, the coupling between diffusion processes in the background and fracture is weak.

Note that in equation (8) for upper cross-over frequency ω_M there is no explicit dependency of the fracture diffusivity. The reason is that in equation (1) fracture properties are lumped into a single parameter that is fracture weakness. Underlying physical reason is the high contrast in spatial scales and compressibilities, which allows simpler parameterization of fractures via fracture weakness parameter. The cross-over frequency ω_M primarily depends on fracture weakness (thickness). It also depends on D_b because the coupling of the two diffusion processes is strong in this case. Since diffusion length in the background is smaller than the diffusion length in fracture, the diffusion process in fracture will be dependent on D_b (amount of fluid that can flow across the interface is influenced by D_b). From equations (6) and (8) we conclude that separation between ω_P and ω_M becomes stronger for smaller fracture weakness and softer fracture matrix.

CONCLUSIONS

We think that results represent a general feature of attenuation due to the so-called mesoscopic flow (in the presence of heterogeneities small compared to the wavelength double-porosity structures. In fact, the three different frequency regimes identified here can be clearly observed in the attenuation behavior of double-porosity configurations as shown in (Pride and Berryman, 2003) and (Pride et al., 2004) (see their Figure 1). Similar intermediate frequency regime is observed in patchy-saturation model (Johnson, 2001) however, properties do not exhibit big contrast, and thus if the spatial scales of fluid patches are very different the overall effect of small heterogeneities is small.

The results derived from equation (1) are limited by the assumption of periodic distribution of fractures. Sensitivity of our results to the violation of the periodicity assumption was examined numerically using reflectivity modeling for layered poroelastic media (Lambert et al., 2005). Numerical experiments for a random distribution of fractures of the same thickness still show good agreement with theoretical results obtained for periodic fractures in a vicinity of the attenuation peak. However, the regime with Q^{-1} proportional to ω is no longer present, and the "intermediate" frequency range with $Q^{-1} \propto \omega^{1/2}$ extends over the low-frequency range. This numerical result for a random distribution of fractures is in agreement with both theoretical and numerical results for randomly layered porous media with small contrast between layers (Gurevich and Lopatnikov, 1985; Gelinsky et al., 1998).

Presented results provide a physical basis for estimation of the reservoir permeability as well as the fracture weakness (thickness) by identifying cross-over frequencies from attenuation measurements. These parameters may provide additional input for reservoir modeling. The major requirement for such an approach is that measurements must be made in over a relatively broad frequency range (between seismic and sonic logging frequencies).

ACKNOWLEDGMENTS

This work was kindly supported by the sponsors of the *Wave Inversion Technology (WIT) Consortium*, Karlsruhe, Germany.

REFERENCES

Bakulin, A., Grechka, V., and Tsvankin, I. (2000). Estimation of fracture parameters from reflection seismic data – Part I: HTI model due to a single fracture set. *Geophysics*, 65:1788–1802.

Brajanovski, M., Gurevich, B., and Schoenberg, M. (2005). A model for p-wave attenuation and dispersion in a porous medium permeated by aligned fractures. *Geophys. J. Int.*, 163:372–384,doi:10.1111/j.1365–246X.2005.02722.x.

Gelinsky, S., Shapiro, S., Müller, T., and Gurevich, B. (1998). Dynamic poroelasticity of thinly layered structures. *Internat. J. Solids Structures.*, 35:4739–4752.

Gurevich, B. and Lopatnikov, S. L. (1985). Attenuation of longitudinal waves in a saturated porous medium with random inhomogeneities. *Doklady Earth Science Sections*, 281:47–50.

Hsu, C. and Schoenberg, M. (1993). Elastic waves through a simulated fractured medium. *Geophysics*, 58:964–977.

Johnson, D. L. (2001). Theory of frequency dependent acoustics in patchy-saturated porous media. *J. Acoust. Soc. Amer.*, 110:682–694.

Lambert, G., Gurevich, B., and Brajanovski, M. (2005). Attenuation and dispersion of p-waves in porous rocks with planar fractures: comparison of theory and numerical simulations. *Geophysics*, Accepted.

Pride, S., Berryman, J. G., and Harris, J. M. (2004). Seismic attenuation due to wave-induced flow. *J. Geophys. Res.*, 109:No. B1, B01201.

Pride, S. R. and Berryman, J. G. (2003). Linear dynamics of double-porosity dual-permeability materials, 1. governing equations and acoustic attenuation. *Physical Review E.*, 68:036603.

Schoenberg, M. and Douma, J. (1988). Elastic-wave propagation in media with parallel fractures and aligned cracks. *Geophys. Prosp.*, 36:571–590.